IEEE Access
Multidisciplinary | Rapid Review | Open Access Journal

Received June 30, 2019, accepted July 7, 2019, date of publication July 11, 2019, date of current version July 30, 2019.

Digital Object Identifier 10.1109/ACCESS.2019.2928274

Enhancing Performances on Wind Power Fluctuation Mitigation by Optimizing Operation Schedule of Battery Energy Storage Systems With Considerations of Operation Cost

XINSONG ZHANG[1], JUPING GU[1], LIANG HUA[1], AND KANG MA[2]
[1]College of Electrical Engineering, Nantong University, Nantong 226019, China
[2]Department of Electronic and Electrical Engineering, University of Bath, Bath BA2 7AY, U.K.

Corresponding author: Juping Gu (gu.jp@ntu.edu.cn)

This work was supported in part by the National Natural Science Foundation of China under Grant 61673226 and Grant 51877112, in part by the Jiangsu Overseas Visiting Scholar Program for University Prominent Young and Middle-Aged Teachers and President, in part by the China Postdoctoral Science Foundation under Grant 2017M611672, and in part by the Natural Science Foundation of the Jiangsu Higher Education Institutions of China under Grant 17KJA470006 and Grant 18KJA470003.

ABSTRACT In this paper, battery energy storage systems (BESSs) are integrated into wind farms (WFs) to mitigate the wind power fluctuations. This paper presents a formulation to optimize the operation schedule of the BESS, with the objective of minimizing the energy of the fluctuating component extracted from the output power of the BESS-integrated WF. The optimal operation schedule of the BESS is utilized to generate the charging/discharging instructions for the BESS to enhance the performances on mitigating the wind power fluctuations. Without proper control, the BESS switches between the charging and discharging states frequently and, thus, degrading batteries significantly, which results in a high operation cost of the BESS. To address this issue, the BESS is divided into two parts, which implement charging and discharging instructions, respectively. Sequential Monte Carlo simulation is applied to simulate the operation of the BESS-integrated WF on a typical day and the simulation results are used to evaluate the technical and economic performances on mitigating the fluctuations. The simulation results validate that the solution can mitigate the output power fluctuations with better performance and a less operation cost than the existing solutions.

INDEX TERMS Battery energy storage systems, operation cost, performances on mitigating the wind power fluctuations, sequential Monte Carlo simulation, wind power fluctuations.

I. INTRODUCTION

As a mature technology, wind generation achieves dramatic progress throughout the world due to energy crisis and environmental issues [1]. Different from conventional generators, the output power of wind farms (WFs) fluctuates inherently because of volatile wind conditions, wind shear and tower shadow [2]. When wind generation penetration is significant in electric power systems, the wind power fluctuations pose great challenges on system operation in many aspects, such as deteriorating power qualities [3], frequency excursions that subsequently increase an extra burden for frequency regulations [4],[5], leading to serious forced oscillations [6], and so on. Therefore, it is desirable to mitigate the wind power fluctuations so that WFs can become not only eco-friendly but also grid-friendly.

Thus far, researchers investigate the fluctuating characteristics of wind power from various perspectives [7]–[11]. In [7], probabilistic characteristics of the fluctuating component extracted from wind power by means of rolling average method are investigated. In [8], the fluctuation of wind power is quantified in the context of frequency controls in power systems. References [9] and [10] indicate that output power fluctuation at the point of common coupling (PCC) of a WF is insignificant compared with that of a single wind turbine generator (WTG) because of geographical smoothing effects.

The associate editor coordinating the review of this manuscript and approving it for publication was Khmaies Ouahada.

Authors of [11] conclude that WF layout affects geographical smoothing effects and thereby has significant impacts on the output power fluctuation at the PCC of a WF. Researches in [7]–[11] can provide support in theory on designing a strategy to mitigate the wind power fluctuations.

One type of methods for mitigating the wind power fluctuations is to exploit the flexibility from WTGs. In [12]–[14], solutions based on pitch angle control and/or control of converters are developed to mitigate the wind power fluctuations. In [15], a hierarchical manner that coordinates dc-link voltage control, rotor speed control, and pitch angle control is developed to mitigate the wind power fluctuations. These solutions have an advantage of implementation simplicity because they do not require any additional devices. However, they cannot consider the geographical smoothing effects pertaining to WFs and may cause individual WTG to deviate from the maximum power tracking point and thus compromising the revenue.

In recent years, battery energy storage technologies achieve significant progress [16], which provides another type of methods to mitigate the wind power fluctuations because battery energy storage systems (BESSs) can respond quickly as required. In [17]–[21], the BESS is employed to mitigate the wind power fluctuations, which is integrated either at the PCC of WF as a BESS-integrated WF or at other point as an independent BESS. In [17], a washout filter-based scheme is developed for the BESS-integrated WF to mitigate the wind power fluctuations, while ensuring state of charge (SOC) of the BESS within a proper range. Reference [18] presents a coordinated control scheme for the BESS-integrated WF to mitigate the output power fluctuations. This scheme extends BESS lifetime by avoiding extreme value of SOC. In [19], a fuzzy-based strategy is designed for the independent BESS to mitigate the wind power fluctuations. However, [17]–[19] do not consider fully how to enhance performances on mitigating the fluctuations in designing operation strategies of the BESS.

In this paper, the BESS is integrated at the PCC of a WF to mitigate the wind power fluctuations. To bridge the gap aforementioned above, a BESS operation schedule optimization model (BOSOM) is proposed, which minimizes the energy of the fluctuating component extracted from the output power of the BESS-integrated WF. On the basis of the updated short-term wind power forecast, the BOSOM is solved every few minutes on a rolling basis to yield an optimal operation schedule for the BESS. The optimal operation schedule of the BESS is utilized to generate the charging/discharging instructions for the BESS, enhancing performances on mitigating the wind power fluctuations.

The BESS will exchange its charging/discharging state frequently in the context of mitigating the wind power fluctuations, which results in a significant battery degradation. The operation cost of the BESS mainly results from the battery degradation, so it can be estimated according to the battery degradation consumed for mitigating the wind power fluctuations [22]. Up to now, batteries are still rather expensive. It is thereby desirable to decrease the battery degradation and the resulted operation cost when the BESS is utilized to mitigate the wind power fluctuations. Reference [20] develops a hybrid energy storage system as the combination of the superconducting energy storage and the BESS to mitigate the wind power fluctuations. The superconducting energy storage is controlled to prevent the BESS from frequent switches between charging and discharging states, thus delaying the battery degradation significantly. In this case, the operation cost of the BESS can be reduced because it mainly results from the battery degradation. In [21], a similar hybrid energy storage system is developed, in which the ultra-capacitor and the BESS are respectively to mitigate short-term and long-term wind power fluctuations. The operation cost of the BESS resulted from the battery degradation can be reduced significantly because the BESS is only used to mitigate long-term wind power fluctuations. However, solutions developed in [20] and [21] require more additional devices and more complex control strategies.

To address the issue aforementioned above, the BESS deployed for mitigating the wind power fluctuations is divided into two separate parts in this paper. Two parts of the BESS are controlled in opposite charging/discharging state to implement charging and discharging instructions respectively. In operations, two parts of the BESS exchange their charging/discharging states simultaneously if any part of the BESS is fully discharged or discharged. In this strategy, battery degradation can be relieved and the operation cost of the BESS can consequently be reduced because frequent state exchanges between charging and discharging are avoided.

The rest of the paper is organized as follows. Section II describes the topology of the BESS-integrated WF and the method of extracting the fluctuating component from output power of the BESS-integrated WF. Section III is devoted to introduce a new solution that can enhance performances on mitigating the fluctuations while reducing the operation cost of the BESS. In Section IV, Sequential Monte Carlo simulation (SMCS) is used to simulate the operation of the BESS-integrated WF. Based on the simulation results, the technical and economic performances on mitigating the fluctuations are quantified in terms of three specially designed indices. Simulation based on a real WF is carried out in Section V to validate the solution proposed in this paper. Section VI concludes the paper.

II. INTRODUCTIONS OF THE BESS-INTEGRATED WF

A. TOPOLOGY OF THE BESS-INTEGRATED WF

In this paper, the BESS is integrated at the PCC of a WF to mitigate the wind power fluctuations, as illustrated in Fig. 1. It is noted in Fig.1 that the BESS is divided into two parts, which are integrated separately through a special DC/AC power converter. The reasons for adoption of this topology to constitute the BESS-integrated WF will be explained in Section III.C.

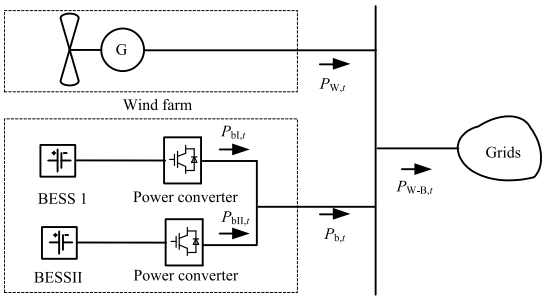

FIGURE 1. BESS-integrated WF schematic diagram.

In Fig.1, $P_{w,t}$ is an output power of the WF at minute t, which is the total output power of all WTGs operated in the WF, $P_{b,t}$ is a charging/discharging power of the BESS at minute t, which is a sum of charging/discharging power of BESSs I and II, denoted here respectively as $P_{bI,t}$ and $P_{bII,t}$. If BESS I/II delivers stored energy to grids, the value of $P_{bI,t}/P_{bII,t}$ is positive, while negative when BESS I/II is absorbing energy from grids. $P_{w-B,t}$ is an output power of the BESS-integrated WF at minute t, which is a sum of the wind power and the BESS charging/discharging power and can be expressed as

$$P_{W\text{-}B,t} = P_{w,t} + P_{b,t} = P_{w,t} + P_{bI,t} + P_{bII,t} \quad (1)$$

B. EXTRACTIONS OF THE FLUCTUATIONS FROM THE OUTPUT POWER OF THE BESS-INTEGRATED WF

The rolling average method is originally designed to separate regulation and load-following components from power load series [23]. In [7], it is extended to extract the fluctuating component from wind power series. In this paper, it is adopted to decompose the output power of the BESS-integrated WF into two parts: a fluctuating component and a continuous component.

The fluctuating component extracted from the output power of the BESS-integrated WF can be expressed as

$$P_{m,t} = P_{w,t} + P_{b,t} - \sum_{i=1}^{N} (P_{w,t-N/2+i} + P_{b,t-N/2+i}) \Big/ N \quad (2)$$

In (2), $P_{m,t}$ is the fluctuating component at minute t, N is a preassigned length of rolling-average time in minutes. The summing part of (2) is an average output power of the BESS-integrated WF from minutes t-$N/2$+1 to $t + N/2$, which is the continuous component at minute t. The length of rolling-average time is a crucial parameter when extracting the fluctuating component from the output power of the BESS-integrated WF, which depends on control area and should be chosen carefully. If the length of rolling-average time is too short, the fluctuations will show up in the continuous components, on the contrary, long-term trends will appear in the fluctuations. In this paper, the length of rolling-average time is set to be 30 minutes as did in [7] and [24].

III. SOULUTIONS OF MITIGATION THE FLUCTUATIONS BY THE BESS

For the BESS-integrated WF illustrated in Fig.1, the output power fluctuations can be mitigated by adjusting charging/discharging power of the BESS. A new solution is developed to mitigate the output power fluctuations with a better performance and a less operation cost than existing solutions, which is briefly illustrated in Fig. 2.

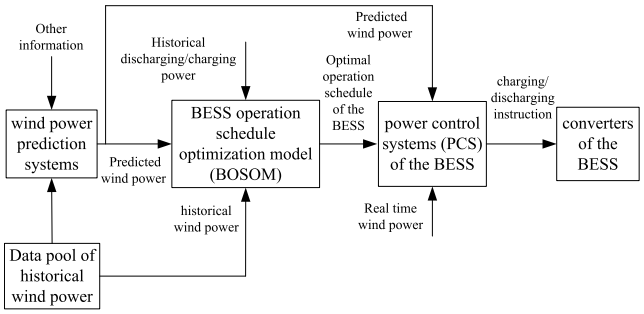

FIGURE 2. Schematic diagram of the solution developed to mitigate the output power fluctuations.

To enhance performance on mitigating the fluctuations, the BOSOM is solved every few minutes to optimize operation schedule of the BESS for an upcoming period on the basis of historical wind power, historical BESS charging/discharging power and predicted wind power. The charging/discharging instructions can then be generated by power control systems (PCS) of the BESS according to the optimal operation schedule of the BESS, real wind power and predicted wind power. Next, two parts of the BESS implement the charging and discharging instructions respectively to avoid frequent switches between charging and discharging states, thus reducing the operation cost of the BESS resulted from the battery degradation. The solution for mitigating the wind power fluctuations will be detailed below.

A. BESS OPERATION SCHEDULE OPTIMIZATION MODEL (BOSOM)

Equation (2) depicts that the fluctuating component at minute t is jointly determined by charging/discharging power of the BESS from minutes t-$N/2$+1 to $t + N/2$ rather than only determined by charging/discharging power of the BESS at present minute. It can also be concluded from (2) that charging/discharge power of the BESS at minute t affects the fluctuations from minutes t-$N/2$ to t+$N/2$+1 simultaneously. Under this condition, if charging/discharging power of the BESS is optimized only aiming to minimize the fluctuating component at present minute, the fluctuations at other minutes might conversely become more serious. And therefore, the BOSOM which minimizes the energy of the fluctuating component during a preassigned time period is presented in this paper to optimize operation schedule of the BESS.

The minimization objective of the BOSOM is expressed as

$$\min E_{\mathrm{h},t} = \sum_{j=0}^{M-1} \left|P_{\mathrm{m},t+j}\right| \Big/ 60 \tag{3}$$

where, $P_{\mathrm{m},t+j}$ is the fluctuating component at minute $t+j$, $E_{\mathrm{h},t}$ is the energy of the fluctuating component from minutes t to $t+M$-1. The period from minutes t to $t+M$-1 is a preassigned time period when optimizing operation schedule of the BESS at minute t-1. Parameter M has direct impacts on optimal operation schedules of the BESS and should be carefully selected by operators.

For a clear description, the minimization objective $E_{\mathrm{h},t}$ is expressed in an abstract form, illustrated as below.

$$\min E_{\mathrm{h},t} = f(P_{\mathrm{b},t+k}, P_{\mathrm{fw},t+k}, P_{\mathrm{b},t+l}, P_{\mathrm{w},t+l}) \tag{4}$$

In (4), variable k indexes future minutes and varies from 0 to $M+N/2$-1. $P_{\mathrm{b},t+k}$ denotes charging/discharging power of the BESS from minutes t to $t+M+N/2$-1, which are decision variables of the BOSOM. $P_{\mathrm{fw},t+k}$ denotes predicted wind power from minutes t to $t+M+N/2$-1, which can be provided by wind power prediction systems (WPPS) according to historical wind power and other information. It is obvious that predicted wind power is prerequisite when optimizing the operation schedules of the BESS. Variable l indexes past minutes and varies from $-N/2+1$ to -1. $P_{\mathrm{w},t+l}$ and $P_{\mathrm{b},t+l}$ are respectively historical wind power and charging/discharging power of the BESS from minutes t-$N/2$+1 to $t-1$, which provide necessary data for the BOSOM.

Constraints of the BOSOM are listed as follow.

1) CONSTRAINT ON CHARGING/DISCHARGING RATES

Excessive charging/discharging rates of the BESS damage batteries significantly. Therefore, charging/discharging rates of the BESS are bounded in the BOSOM, illustrated as (5).

$$\begin{cases} P_{\mathrm{b},t} \le E_{\mathrm{c}} P_{\mathrm{dism}} & P_{\mathrm{b},t} > 0 \\ \left|P_{\mathrm{b},t}\right| \le E_{\mathrm{c}} P_{\mathrm{chm}} & P_{\mathrm{b},t} < 0 \end{cases} \tag{5}$$

In operation, BESSs I and II are controlled in opposite charging/discharging states and implement charging and discharging instructions respectively. If a charging instruction is generated, a part of the BESS that is in charging state responds it immediately, in contrast, another part of the BESS is idle at this moment because it is in discharging state. If a discharging instruction is generated, similar situation occurs. It can be deduced that only one part of the BESS will be in operations no matter what charging/discharging instructions are generated. Therefore, E_{c} in (5) is set to be the capacity of BESS I/II rather than the capacity of whole BESS. P_{chm} and P_{dism} are respectively maximum charging and discharging rate of the BESS with unit capacity (i.e., 1 MWh), which mainly depend on the battery characteristics.

2) CONSTRAINT ON STATE OF CHARGE

The BESS will suffer significant lifetime deterioration if being over charged or discharged. For this reason, the SOC of the BESS is required to be stay with a preassigned range, illustrated as below.

$$V_{\mathrm{mins}} \le V_{\mathrm{soc},t} \le V_{\mathrm{maxs}} \tag{6}$$

In (6), V_{maxs} and V_{mins} are respectively maximum and minimum values of the SOC, which mainly depend on types of batteries. $V_{\mathrm{soc},t}$ is in fact a fictitious SOC at the end of minute t because two parts of the BESS implement charging and discharging instructions respectively, which can be calculated by

$$V_{\mathrm{soc},t} = \begin{cases} V_{\mathrm{soc},t-1} - P_{\mathrm{b},t} \big/ [60\eta_{\mathrm{dis}} E_{\mathrm{c}}] & P_{\mathrm{b},t} \ge 0 \\ V_{\mathrm{soc},t-1} - [P_{\mathrm{b},t}\eta_{\mathrm{ch}}] \big/ [60E_{\mathrm{c}}] & P_{\mathrm{b},t} < 0 \end{cases} \tag{7}$$

In (7), η_{ch} and η_{dis} are respectively charging and discharging efficiency coefficients of the BESS, which mainly depend on the type of batteries.

B. CHARGING/DISCHARGING INSTRUCTIONS OF THE BESS

The BOSOM described above is a non-convex optimization problem because the objective function illustrated as (3) is an accumulation of absolute values. This type of optimization problem can easily be transformed into a mixed integer linear programming (MILP) problem by introducing binary variables, which can directly be solved by CPLEX solver in General Algebraic Modeling System (GAMS) environment [25].

On the basis of historical wind power and charging/discharging power of the BESS, the BOSOM is solved every M minutes in a rolling way according to updated short-term predicted wind power. In practice, short-term predicted wind power is updated to give more accurate results every several minutes. In order to utilize latest short-term predicted wind power, solution of the BOSOM should keep path with the update of short-term predicted wind power. That is to say, parameter M can be determined according to update frequency of short-term predicted wind power. For example, if short-term predicted wind power is updated every 30 minutes, the BOSOM is also solved every 30 minutes, i.e., the value of parameter M is set to be 30.

If the BOSOM is solved at minute t-1, it can give the optimal operation schedule of the BESS from minutes t to $t+M+N/2$-1. However, only part of the operation schedule that is from minutes t to $t+M$-1 is transferred to the PCS of the BESS for generating charging/discharging instructions of the BESS. As for the operation schedule from minutes $t+M$ to $t+M+N/2$-1, it is given in next solution of the BOSOM that is scheduled at minute $t+M$-1.

Based on the optimal operation schedule of the BESS, the PCS of the BESS can generate charging/discharging instructions for the BESS. If wind power can be predicted perfectly, desired performance on mitigating the fluctuations can be achieved as long as the BESS operates as the operation schedule optimized by the BOSOM. Although engineers took great efforts to improve predicting technologies [26], it is

still impossible to predict wind power accurately even the predicting lead time is short. Under this condition, the BESS should not only follow the operation schedule optimized by the BOSOM but also compensate random power mismatches between predicted wind power and real wind power. At minute t, the charging/discharging instruction of the BESS denoted here as $P_{\mathrm{db},t}$ can be calculated as

$$P_{\mathrm{db},t} = P_{\mathrm{sb},t} + P_{\mathrm{fw},t} - P_{\mathrm{w},t} \tag{8}$$

where, $P_{\mathrm{sb},t}$ is a charging/discharging rate fixed in the operation schedule; $P_{\mathrm{fw},t} - P_{\mathrm{w},t}$ is a random power mismatch between real wind power and predicted wind power at minute t. If the parameter M is not determined according to update frequency of short-term predicted wind power, the latest short-term predicted wind power (i.e., most accurate short-term predicted wind power) cannot be utilized by the BOSOM to optimize the operation schedule of the BESS. In this case, charging/discharging power of the BESS required to compensate power mismatches between predicted wind power and real wind power increases, thus accelerating the battery degradation.

C. IMPLEMENTATIONS OF THE CHARGING/DISCHARGING INSTRUCTION BY TWO PARTS OF THE BESS

A part of the operation schedule of the BESS optimized by the BOSOM is illustrated in Fig. 3, in which the BESS switches 5 times between charging and discharging states during 4 hours. The switching times of the BESS between charging and discharging states cannot be predetermined in the BOSOM, in contrast, they are counted according to the operation schedule of the BESS optimized by the BOSOM. It is emphasized that this operation schedule is optimized by solving the BOSOM several times rather than only one time. For example, if length of the studied horizon is set to be 30 minutes (i.e., the value of parameter M is set to be 30), this operation schedule is optimized by solving the BOSOM 8 times.

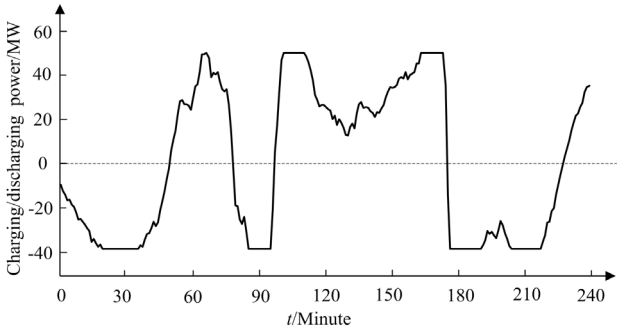

FIGURE 3. Optimal operation schedule of the BESS during certain 4 hours.

It can be found from (4) that the BOSOM is devoted to enhance performances on mitigating the wind power fluctuations as far as possible by optimizing the operation schedule of the BESS. However, the operation cost of the BESS is not considered in this process. As a result, the BESS might switch between charging and discharging states frequently when operating as the optimal operation schedule, thus increasing the operation cost of the BESS. For example, the BESS switches 5 times between charging and discharging states during 4 hours, as illustrated in Fig. 3. More seriously for the BESS, it could switch its state more times in operation, because it not only follows the optimal operation schedule but also compensates random predicted errors on wind power to achieve desired performances on mitigating the fluctuations. Frequent switches of the BESS between charging and discharging states degrade batteries significantly, thus resulting in a high operation cost of the BESS.

To address the issue described above, the BESS is divided into two parts with identical characteristic and capacity, as illustrated in Fig. 1. In operations, two parts of the BESS are controlled at opposite charging/discharging states and implement charging and discharging instructions respectively. In other words, one part of the BESS in state of charging implements charging instructions, in contrast, another part of the BESS is in discharging state and meets discharging requirements. Under this condition, the capacity requirement and resulting investment cost of the BESS are all double if rated charging/discharging power of the BESS remains unchanged. Fortunately, switches of the BESS between charging and discharging states can be reduced significantly, thus delaying the battery degradation. The operation cost of the BESS mainly results from the battery degradation, therefore, the strategy proposed in this paper might save the operation cost of the BESS even if the investment cost of the BESS is double.

For convenience of descriptions, BESS I is assumed to be at charging state at minute t. Meanwhile, BESS II is in state of discharging according to the operation strategy designed for the BESS. At minute t, if a charging instruction is generated by the PCS of the BESS (i.e., the value of $P_{\mathrm{db},t}$ is negative), BESS I should implement it immediately as it is just in charging state. On the contrary, BESS II in state of discharging will stand by and get ready to respond the discharging instruction possibly generated in next minute. However, BESS I might not meet the charging requirement entirely because it must avoid damages resulted from excessive charging rate and overcharging. At this time, the charging power of BESS I can be determined as below.

$$P_{\mathrm{bI},t} = -\min[-P_{\mathrm{db},t}, P_{\mathrm{cmaxI},t}] \tag{9}$$

In (9), $P_{\mathrm{cmaxI},t}$ is a maximum charging rate that BESS I can provide at minute t, which depends on not only technical characteristics of batteries but also the SOC of BESS I at the end of previous minute, and can be calculated as

$$P_{\mathrm{cmaxI},t} = \min[E_{\mathrm{c}}P_{\mathrm{chm}}, 60E_{\mathrm{c}}(V_{\mathrm{maxs}} - V_{\mathrm{socI},t-1})/\eta_{\mathrm{ch}}] \tag{10}$$

where $V_{\mathrm{socI},t-1}$ is the SOC of BESS I at the end of minute t-1, the first item in the bracket limits charging rate to avoid damages from excessive charging rates, and the second item in the bracket prevents overcharging to deteriorate batteries. At the end of minute t, the SOC of BESS II remains unchanged

because BESS II is idle at present minute, while the SOC of BESS I is updated as

$$V_{\mathrm{socI},t} = V_{\mathrm{socI},t-1} - [P_{\mathrm{bI},t}\eta_{\mathrm{ch}}]/[60E_{\mathrm{c}}] \tag{11}$$

where $V_{\mathrm{socI},t}$ is the SOC of BESS I at the end of minute t.

In contrast, BESS II being in discharging state will respond immediately provided the PCS of the BESS gives a discharging instruction at minute t, i.e., the value of $P_{\mathrm{db},t}$ is greater than zero. Excessive discharge rates and over discharging damage batteries, so BESS II might not meet discharging requirement entirely. At present minute, the discharging power of BESS II can be determined as below.

$$P_{\mathrm{bII},t} = \min[P_{\mathrm{db},t}, P_{\mathrm{dmaxII},t}] \tag{12}$$

In (12), $P_{\mathrm{dmaxII},t}$ is a maximum discharging rate that BESS II can provide at minute t, which depends on technical characteristics of batteries as well as the SOC of BESS II at the end of previous minute, and can be calculated as

$$P_{\mathrm{dmaxII},t} = \min[E_{\mathrm{c}}P_{\mathrm{dism}}, 60E_{\mathrm{c}}(V_{\mathrm{socII},t-1} - V_{\mathrm{mins}})\eta_{\mathrm{dis}}] \tag{13}$$

where $V_{\mathrm{socII},t-1}$ is the SOC of BESS II at the end of minute t-1, the first item in the bracket bounds discharging rate to prevent excessive discharging rates to deteriorate batteries, and the second item in the bracket is employed to avoid over discharging because it can also damage batteries. At the end of present minute, the SOC of BESS I remains unchanged because BESS I is idle at present minute, while the SOC of BESS II is updated by

$$V_{\mathrm{socII},t} = V_{\mathrm{socII},t-1} - [P_{\mathrm{bII},t}]/[60\eta_{\mathrm{dis}}E_{\mathrm{c}}] \tag{14}$$

where $V_{\mathrm{socII},t}$ is the SOC of BESS II at the end of minute t.

From (9)-(14), it can be concluded that it is necessary to ensure that two parts of the BESS have identical characteristics and capacities. If not, the maximum charging/discharging rate that the BESS can provide and real charging/discharging power of the BESS depend on which part of the BESS is in charging/discharging state, thus possibly degrading performances on mitigating the wind power fluctuations.

At the end of minute t, if any part of the BESS is fully charged or discharged, its state must be changed immediately to avoid damages from over charging or discharging. As for another part of the BESS, it also changes its state simultaneously no matter what its SOC, as illustrated in Fig. 4. If that is the case, two parts of the BESS can be guaranteed to stay in different charging/discharging states at any time. For example, BESS I is in discharging state from minute t_1 to t_2, while BESS II is in charging state during this period. Under this condition, the BESS has potential to respond any power instructions generated by the PCS of the BESS. However, the BESS cannot always execute the power instructions completely because the charging/discharging power of the BESS is limited by rated charging/discharging rate and maximum/minimum value of the SOC (i.e., maximum/minimum energy that the BESS can store). For example, if the PCS of the BESS gives a charging instruction at minute t_1, BESS I responds it immediately because it is just in charging state. However, BESS I is not capable of executing it completely when the amplitude of the charging instruction is too large, because the charging power that BESS I can provide at minute t_1 is limited by rated charging rate and maximum value of the SOC.

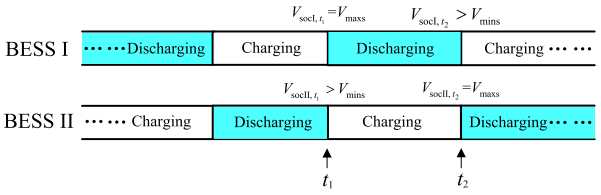

FIGURE 4. State exchanging of two parts of the BESS.

In Fig. 4, BESS I is fully charged at the end of minute t_1, i.e., its SOC arrives the maximum value V_{maxs}. At this moment, it must be changed to discharging state immediately to prevent over charging. Meanwhile, BESS II is changed from discharging state to charging state simultaneously although it does not discharge fully. At the end of minute t_2, BESS II is fully charged and consequently changes to discharging state. At this moment, BESS I is changed from discharging state to charging state along with BESS II to ensure that two parts of the BESS always stay in opposite charging/discharging state. The strategy described above can reduce the switches between charging and discharging states of the BESS, in which reduction of the switches between charging and discharging is not related to depth of charge/discharge directly but related to maximum and minimum SOC of the BESS.

IV. ASSESSMENTS OF PERFORMANCES ON MITIGATING THE FLUCTUATIONS BASED ON SEQUENTIAL MONTE CARLO SIMULATIONS

A. INDICES

In this paper, two indices are specifically designed to quantify technical performances on mitigating the fluctuations respectively from two aspects: one is from the fluctuating energy and the other is from the fluctuating power amplitude. These two indices are respectively a percentage of mitigated fluctuating energy (PMFE) and a probability of fluctuation exceeding a threshold (PFET).

The index PMFE quantifies the energy of the fluctuating component that has be mitigated by the BESS on a dispatching day in terms of percentage, which can be calculated as

$$V_{\mathrm{PMFE}} = \frac{\frac{1}{60}\left\{\sum_{t=1}^{1440}\left|P_{\mathrm{wm},t}\right| - \sum_{t=1}^{1440}\left|P_{\mathrm{m},t}\right|\right\}}{\frac{1}{60}\sum_{t=1}^{1440}\left|P_{\mathrm{wm},t}\right|} \times 100\% \tag{15}$$

In (15), V_{PMFE} is a value of the index PMFE; $P_{\mathrm{wm},t}$ is a fluctuating component at minute t extracted from the wind power, which can be calculated by (2) provided $P_{\mathrm{b},t}$ is set to be zero. It is obvious that the denominator of (15) is the energy of the fluctuating component extracted from the wind

power on the dispatching day, which provides a benchmark to calculate the index PMFE.

The index PFET gives an occurrence probability of the event that the amplitude of the fluctuating component exceeds a predefined threshold on a dispatching day, which can be calculated as

$$V_{\mathrm{PFET}} = P_{\mathrm{r}}\left\{\left|P_{\mathrm{m},t}\right| > P_{\mathrm{thr}}\right\} \quad t = 1,\ 2, \ldots,\ 1440 \tag{16}$$

In (16), V_{PFET} is a value of the index PFET; $P_{\mathrm{r}}\{\}$ is an occurrence probability of the event given in the bracket; P_{thr} is a predetermined threshold of the fluctuating power.

At present, the batteries are still rather expensive, which makes it necessary to evaluate the operation cost of the BESS. An index entitled as expected operation cost of the BESS (EOCB) is designed to quantify the operation cost of the BESS consumed for mitigating the fluctuations. In [22], BESS is adopted to ensure that WF can trace the desired generation schedules and the operation cost of the BESS is calculated according to the battery degradation. In this paper, the operation cost of the BESS is also calculated as the method proposed in [22], which can be expressed as

$$V_{\mathrm{EOCB}} = [E_{\mathrm{c}} V_{\mathrm{invest}}(n_1 + n_2)] \big/ [2n_{\mathrm{total}}] \tag{17}$$

In (17), V_{EOCB} is a value of the index EOCB; n_{total} is the number of charge-discharge cycles the BESS can undertake over its useful lifetime, which mainly depend on types of batteries; n_1/n_2 is the number of charge-discharge cycles BESS I/II undertaken over a dispatching day; V_{invest} is an investment cost of the BESS with unit capacity.

B. THE OPERATION SIMULATION OF THE BESS-INTEGRATED WF

The fluctuating component at minute t is jointly determined by charging/discharging power of the BESS from minutes t-N/2+1 to $t + N/2$, as illustrated in (2). On the other hand, charging/discharging power of the BESS at minute t affects the fluctuations not only at minute t but also from minutes t-N/2 to $t+N/2$+1. In addition, maximum available charging/discharging rate provided by the BESS at minute t depends on the SOC at the end of previous minute, as illustrated in (10) and (13). As mentioned above, the operation of the BESS-integrated WF is of significant chronological character, which must be considered in the operation simulation. In addition, wind power forecast errors affect the operation of the BESS-integrated WF significantly, which must also be included in the operation simulation.

In this paper, SMCS is employed to simulate the operation of the BESS-integrated WF on a preassigned dispatching day, because it can not only consider random forecast errors on wind power but also easily model chronological characteristics [27]. Simulation steps are detailed as follows,

Step 0: The index of simulation, denoted here as m is initialized to be 1. Indices PMFE, PFET and EOCB are initialized to be zero.

Step 1: The index of minute is set to be zero, i.e., let $t = 0$. BESSs I and II are initialized to be at charging and discharging states respectively, and the SOC of them are initialized to be V_{mins} and V_{maxs} respectively. On the basis of historical wind power, historical charging/discharging power of the BESS and predicted wind power, the BOSOM is solved by CPLEX solver in GAMS environment to obtain the operation schedule of the BESS from minutes 1 to M. It is pointed out that the BOSOM will be solved every M minutes to optimize the operation schedule of the BESS for upcoming M minutes, i.e., it will be repeatedly solved at minute M, minute $2M$, …, and minute $([1440/M]-1)M$.

Step 2: let $t = t+1$. Real wind power at minute t is assumed to obey a normal distribution in this paper. Under this assumption, randomly generate a wind power at minute t by

$$P_{\mathrm{w},t} = P_{\mathrm{fw},t} + \sigma_t \sqrt{-2\log c_1}\cos 2\pi c_2 \tag{18}$$

where σ_t is a standard deviation of the normal distribution describing random character of the wind power; c_1 and c_2 are two uniformly-distributed random number in [0, 1], which are utilized to generate a random number that obeys standardized normal distribution by means of Box-Muller.

Step 3: Generate a charging/discharging instruction at minute t for the BESS according to (8) and subsequently calculate charging/discharging rates of BESSs I and II respectively by (9) and (12).

Step 4: Calculate the SOC of BESSs I and II at the end of minute t respectively by (11) and (14). If any part of the BESS charges or discharges fully (i.e., its SOC arrives V_{maxs} or V_{mins}), BESSs I and II switch their charging/discharging states immediately. The BOSOM is solved to optimize the operation schedule of the BESS during upcoming M minutes if minute index t arrives at $M, 2M, \ldots,$ and $([1440/M]-1)M$.

Step 5: Repeat steps 2-4 until the dispatching day is entirely covered and subsequently calculate indices PMFE, PFET and EOCB with respect to present simulation according to (15), (16) and (17), denoted here as $V_{\mathrm{PMFE},m}$, $V_{\mathrm{PFET},m}$ and $V_{\mathrm{EOCB},m}$ respectively. And then update indices PMFE, PFET and EOCB respectively as

$$V_{\mathrm{PMFE}} = V_{\mathrm{PMFE}} + V_{\mathrm{PMFE},m} \big/ n_{\max} \tag{19}$$

$$V_{\mathrm{PFET}} = V_{\mathrm{PFET}} + V_{\mathrm{PFET},m} \big/ n_{\max} \tag{20}$$

$$V_{\mathrm{EOCB}} = V_{\mathrm{EOCB}} + V_{\mathrm{EOCB},m} \big/ n_{\max} \tag{21}$$

where $n_{\max}$ is a predetermined maximum simulation time, which should be large enough to guarantee the coefficient of variation is less than the specified tolerance error.

Step 6: Let $m = m+1$ and repeat steps 1-5 until the maximum simulation time is arrived.

V. CASE STUDY

A WF with a capacity of 575 MW is selected as a case WF in this paper. Some simulations will be executed based on a typical dispatching day of the case WF to validate the solutions designed for mitigating the wind power fluctuations. The typical dispatching day is selected from 2017 and the

wind power fluctuating characteristics on which are of universality not only from the aspect of fluctuating energy but also from the aspect of fluctuating power amplitudes.

A. PARAMETERS OF THE CASE

Wind power of the case WF on the dispatching day is illustrated in Fig. 5, total energy of which is 3416.84 MWh. The fluctuating and continuous components extracted from the wind power are respectively given in Fig. 6 with different colors. The energy of the fluctuating component illustrated in Fig. 6 is 149.303 MWh, which accounts for 4.37% of the total energy and provides a benchmark to calculate the index PMFE. On the dispatching day, probabilities of the events that the amplitude of the fluctuating component exceeds a series of thresholds are illustrated in Fig. 7, which are values of the index PFET with respect to these thresholds.

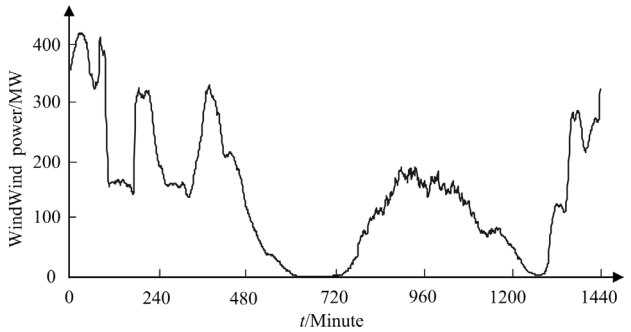

FIGURE 5. Wind power of the case WF on the dispatching day.

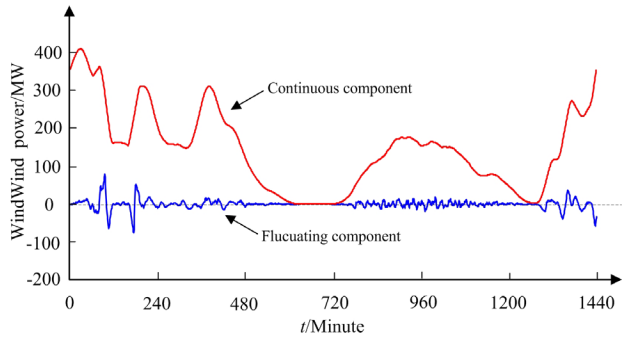

FIGURE 6. Fluctuating and continuous components extracted from wind power of the case WF on the dispatching day.

To mitigate the wind power fluctuations, a BESS with a capacity of 200 MWh is integrated at the PCC of the case WF as the topology illustrated in Fig.1, i.e., the capacities of BESSs I and II are all 100 MWh. Technical and economic parameters of the BESS with unit capacity (i.e., 1 MWh) are illustrated in Table 1 [22].

The standard deviation of the normal distribution describing random character of wind power is set to be 2 percent of predicted wind power. When simulating the operation of the BESS-integrated WF by the SMCS, simulation times are set to be 10^6 for achieving adequately accurate results.

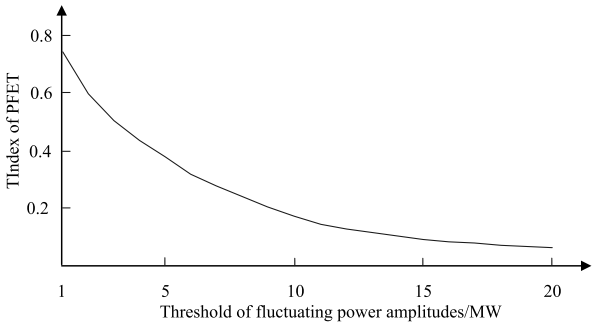

FIGURE 7. The index of PFET of the case WF on the dispatching day.

TABLE 1. Technical and economic parameters of the BESS with unit capacity.

Parameters	Values
Rated charging power/MW	0.39
Rated discharging power/MW	0.5
Charging Efficient	95%
Discharging Efficient	95%
Maximum value of SOC	0.8
Minimum value of SOC	0.2
Life circle/times	2×10^4
Cost/ ¥	5×10^6

In the case WF, short-term predicted wind power is updated every 30 minutes, so the value of parameter M is set to be 30 accordingly.

B. EFFECTIVENESS OF THE BESS OPERATION SCHEDULE OPTIMIZATION MODLE

In this paper, the BOSOM optimizes the operation schedule of the BESS every M minutes, which can be utilized to generate the charging/discharging instructions of the BESS for enhancing performances on mitigating the fluctuations. With the help of the BOSOM, the energy of the fluctuating component extracted from the output power of the BESS-integrated WF decreases from 149.303 MWh to 57.35 MWh on the dispatching day. That is to say, 61.6 percent of the energy of the fluctuating component has been mitigated by the BESS, i.e., the value of index PMFE is 61.6% on the dispatching day.

For comparisons, the charging/discharging instructions of the BESS are assumed to be generated without adopting the operation schedule optimized by the BOSOM. Under this assumption, the BESS charging/discharging instruction at minute t can be generated as

$$\begin{cases} P_{\mathrm{db},t} = -\left(P_{\mathrm{w},t} - P_{\mathrm{c},t}\right) \\ P_{\mathrm{c},t} = \left[\sum_{i=1}^{N/2-1}\left(P_{\mathrm{w},t-N/2+i} + P_{\mathrm{b},t-N/2+i}\right) + P_{\mathrm{w},t} + \sum_{i=1}^{N/2} P_{\mathrm{wf},t+i}\right]/N \end{cases} \tag{22}$$

where, $P_{\mathrm{c},t}$ is a continuous component at minute t extracted from the output power of the BESS-integrated WF. The BESS

is only controlled to compensate the fluctuating component at present minute as far as possible if the charging/discharging instruction of the BESS is generated according to (22). Under this assumption, the energy of the fluctuating component extracted from the output power of the BESS-integrated WF increases from 57.35 MWh to 72.60 MWh, i.e., the index PMFE deteriorates from 61.6% to 51.3% correspondingly.

For the BESS-integrated WF, probabilities of the events that the amplitude of the fluctuating component exceeds a series of thresholds on the dispatching day (i.e., the values of index PFET with these thresholds on the dispatching day) with and without adopting the BOSOM are respectively illustrated in Fig. 8 in different colors. The values of index PFET with different thresholds before the BESS is integrated into the case WF are also illustrated in the same figure with dotted line. Fig. 8 depicts that the index PFET of the BESS-integrated WF has an advantage over that of the case WF in all thresholds no matter the BOSOM is utilized to generate the charging/discharging instructions of the BESS or not. In addition, the index PFET becomes better on the whole if the charging/discharging instructions of the BESS are generated according to the operation schedule of the BESS optimized by the BOSOM. If the BOSOM is solved at minute t-1, it optimizes the operation schedule of the BESS to minimize the energy of the fluctuating component from minutes t to t+M-1 rather than only minimize the fluctuating power at present minute. In contrast, the object is just to minimize fluctuating power at present minute if the charging/discharging instructions are generated directly according to (22). Therefore, adoptions of the operation schedule of the BESS optimized by BOSOM to generate charging/discharging instructions conversely make the index PFET worse slightly when the threshold becomes larger, as illustrated in Fig. 8.

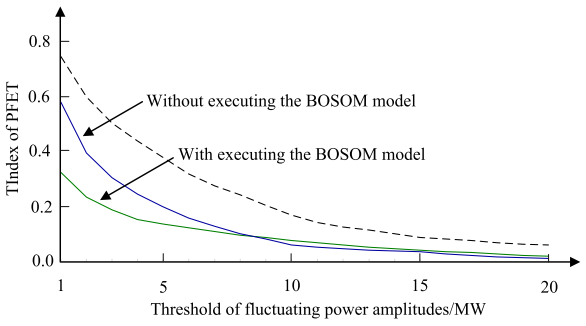

FIGURE 8. The index of PFET on the dispatching day with and without executing the BOSOM.

As mentioned above, the BESS can enhance performance on mitigating the wind power fluctuations not only from the aspect of fluctuating energy but also from the aspect of fluctuating power amplitudes if it operates according to the solution developed in this paper.

C. EFFECTIVENESS OF OPERATION STRATEGY DESIGNED FOR TWO PARTS OF THE BESS

In the case study, parameter M is set to be 30, so the BOSOM is solved at minute 0, minute 30, minute 60, …, and minute 1410 respectively to optimize the operation schedule of the BESS for next 30 minutes, which is utilized to generate power instructions of the BESS. Two parts of the BESS are controlled at opposite charging/discharging states and implement the charging and discharging instructions respectively. To show the operation strategy of the BESS intuitively, we present the SOC of BESSs I and II during the first 4 hours on the dispatching day in Fig. 9. Two curves illustrated in Fig. 9 are generated according to certain simulation in the SMCS. The initial states of BESSs I and II are respectively charging and discharging state, and initial SOC of them are respectively equal to minimum and maximum values of SOC (i.e., 0.2 and 0.8).

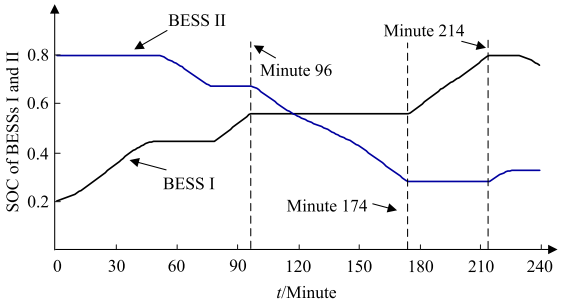

FIGURE 9. SOC of BESS I and BESS II during the first 4 hours on the dispatching day in certain simulation.

Fig. 9 depicts that if one part of the BESS implements charging/discharging instructions, another part of the BESS is idle and its SOC remains unchanged. For example, the PCS of the BESS gives a discharging instruction from minute 96 to minute 174, during this period, BESS II being in discharging state responds it and discharges to the grid, while BESS I is idle because it is in charging state. In operations, charging/discharging states of two parts of the BESS switch simultaneously, if and only if any part of the BESS is fully charged/discharged. It can therefore be concluded that during every 30 minutes starting respectively from minute 0, minute 30, minute 60, …, and minute 1410, charging/discharging state of each part of the BESS remains unchanged unless any part of the BESS is fully charged/discharged during this period. At minute 214, BESS I is fully charged and changes to discharging state, meanwhile BESS II changes from discharging state to charging sate simultaneously in spite of the fact that BESS II does not discharge fully yet. That is to say, charging/discharging state of each part of the BESS changes during the period from minute 210 to minute 240. After minute 214, if the PCS of the BESS gives a discharging instruction, BESS I responds it and discharges to the grid, while BESS II is idle because it has changed to charging state. From Fig. 9, it can also be found that there is not direct energy

exchange between two parts of the BESS. If one part of the BESS discharges to the grid or absorbs energy from the grid, another part of the BESS is always idle.

If the BESS operates as the strategy proposed in this paper, there is a hope of reducing switches of the BESS between charging and discharging state and consequently reducing the operation cost of the BESS. The numbers of charge-discharge cycles two parts of the BESS undertaken on the dispatching day are both 2.14 if the BESS operates as the strategy designed in this paper. Under the circumstances, the operation cost of the BESS is estimated to be ¥107, 000, i.e., the value of index EOCB is ¥107, 000. For comparison, it is assumed that the BESS is not divided into two parts and implements the charging and discharging instructions as a whole. If the rated charging/discharging power of the BESS remains unchanged, only one part of the BESS (i.e., BESS I or BESS II) is required to mitigate the wind power fluctuations at any time. It can be concluded that the capacity requirement of the BESS reduces from 200 MWh to 100 MWh under this assumption. However, the number of charge-discharge cycles the BESS undertaken on the dispatching day increases remarkably from 2.14 to 15.83. Accordingly, the operation cost of the BESS increases from ¥107, 000 to ¥395, 750, i.e., the index EOCB increases from ¥107, 000 to ¥395, 750. From the comparison described above, it can be concluded that the operation strategy designed for the BESS is effective because it can reduce switches of the BESS between charging and discharging state significantly and consequently reduce the operation cost of the BESS.

D. IMPACTS OF PREDICTIVE PRECISION OF WIND POWER ON MITIGATING THE FLUCTUATIONS

Short-term predicted wind power provides necessary data for the optimization of the BESS operation schedule. This schedule is utilized to generate charging/discharging instructions of the BESS, so random forecast errors on wind power probably have an impact on mitigating the fluctuations. If the standard deviation of the normal distribution describing random character of the wind power increases from 2 percent to 5 percent of the forecasted wind power, the energy of the fluctuating component increases from 57.35 MWh to 63.66 MWh on the dispatching day, i.e., the index PMFE deteriorates from 61.6% to 57.4%. In contrast, the energy of the fluctuating component decreases from 57.35 MWh to 54.26 MWh on the dispatching day (i.e., the index PMFE increases from 61.6% to 63.7%), if wind power can be predicted without errors.

Probabilities of the events that the amplitude of the fluctuating component exceeds a series of thresholds on the dispatching day (i.e., the values of index PFET with these thresholds on the dispatching day) in different predictive precision of wind power are respectively illustrated in Fig. 10 in different colors. Fig. 10 depicts that predictive precision of wind power has a significant impact on the index PFET. When the fluctuating power threshold is small, the index

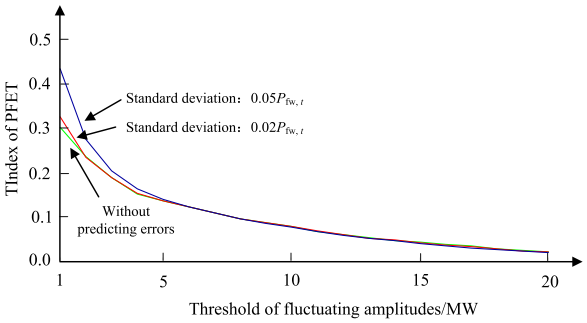

FIGURE 10. The index of PFET in different predictive precision of wind power on the dispatching day.

PFET deteriorates dramatically if predictive precision of wind power gets worse. If the fluctuating component is large enough, the BESS cannot mitigate it entirely because of capacity limitation even if the wind power can be predicted without errors. And therefore, when the threshold is large, the index PFET only changes slightly with predictive precision of wind power, as illustrated in Fig. 10.

In summary, performances on mitigating the fluctuations can be enhanced further if more accurate short-term wind power predicting results are available. Under this condition, to improve wind power prediction technology is appealing when we desire to mitigate the wind power fluctuations by the BESS.

VI. CONCLUSION

In this paper, the solution that can mitigate the fluctuations with a better performance and a less operation cost than existing solutions is investigated. The indices PMFE and PFET are designed to quantify performances on mitigating the fluctuations from two different aspects. In addition, the index EOCB is designed to evaluate the operation cost of the BESS consumed for mitigating the fluctuations. These indices can be calculated according to the simulation results provided by SMCS. A case study on a real WF validates the solution which mitigates the wind power fluctuations. Two main original contributions of this paper are summarized as follows,

1. The BOSOM is presented in this paper, which can be solved by commercial software in a rolling way to optimize the operation schedule of the BESS. If the charging/discharging instructions of the BESS are generated according to the schedule optimized by BOSOM, the performances on mitigating the wind power fluctuations can be enhanced significantly.

2. An effective operation strategy is designed for the BESS, in which the BESS is divided into two parts to implement charging and discharging instructions respectively. The operation strategy can reduce the operation cost of the BESS significantly as it can avoid frequent exchanges of the BESS between charging and discharging states.

REFERENCES

[1] H. Zhao, Q. Wu, S. Hu, H. Xu, and C. N. Rasmussen, "Review of energy storage system for wind power integration support," *Appl. Energy*, vol. 137, pp. 545–553, Jan. 2015.

[2] S. G. Varzaneh, G. B. Gharehpetian, and M. Abedi, "Output power smoothing of variable speed wind farms using rotor-inertia," *Electr. Power Syst. Res.*, vol. 116, pp. 208–217, Nov. 2014. doi: 10.1016/j.epsr.2014.06.006.

[3] F. Girbau-Llistuella, A. Sumper, F. Díaz-González, and S. Galceran-Arellano, "Flicker mitigation by reactive power control in wind farm with doubly fed induction generators," *Int. J. Elect. Power Energy Syst.*, vol. 55, pp. 285–296, Feb. 2014. doi: 10.1016/j.ijepes.2013.09.016.

[4] L. Jin, S. Yuan-zhang, P. Sorensen, L. Guo-Jie, and G. Weng-Zhong, "Method for assessing grid frequency deviation due to wind power fluctuation based on "time-frequency transformation,"" *IEEE Trans. Sustain. Energy*, vol. 3, no. 1, pp. 65–73, Jan. 2012. doi: 10.1109/TSTE.2011.2162639.

[5] B. Cheng and W. B. Powell, "Co-optimizing battery storage for the frequency regulation and energy arbitrage using multi-scale dynamic programming," *IEEE Trans. Smart Grid*, vol. 9, no. 3, pp. 1997–2005, May 2018. doi: 10.1109/TSG.2016.2605141.

[6] C. Su, W. Hu, Z. Chen, and Y. Hu, "Mitigation of power system oscillation caused by wind power fluctuation," *IET Renew. Power Gener.*, vol. 7, no. 6, pp. 639–651, Nov. 2013. doi: 10.1049/iet-rpg.2012.0253.

[7] W. Lin, J. Wen, S. Cheng, and W. Lee, "An investigation on the active-power variations of wind farms," *IEEE Trans. Ind. Appl.*, vol. 48, no. 3, pp. 1087–1094, May/Jun. 2012. doi: 10.1109/TIA.2012.2190817.

[8] T. Ikegami, C. T. Urabe, T. Saitou, and K. Ogimoto, "Numerical definitions of wind power output fluctuations for power system operations," *Renew. Energy*, vol. 115, pp. 6–15, Aug. 2018. doi: 10.1016/j.renene.2017.08.009.

[9] G. McNerney and R. Richardson, "The statistical smoothing of power delivered to utilities by multiple wind turbines," *IEEE Trans. Energy Convers.*, vol. 7, no. 4, pp. 644–647, Dec. 1993. doi: 10.1109/60.182646.

[10] K. Abe, O. Ishioka, Y. Ichikawa, and S. Enomoto, "The analysis of the wind power fluctuation and a consideration of smoothing effect," *IEEJ Trans. Power Energy*, vol. 121, no. 12, pp. 1681–1689, Dec. 2001. doi: 10.1541/ieejpes1990.121.12_1681.

[11] H. Kazari, H. Oraee, and B. C. Pal, "Assessing the effect of wind farm layout on energy storage requirement for power fluctuation mitigation," *IEEE Trans. Sustain. Energy*, vol. 10, no. 2, pp. 558–568, Apr. 2019. doi: 10.1109/TSTE.2018.2837060.

[12] M. A. Chowdhury, N. Hosseinzadeh, and W. X. Shen, "Smoothing wind power fluctuations by fuzzy logic pitch angle controller," *Renew. Energy*, vol. 38, no. 1, pp. 224–233, Feb. 2012. doi: 10.1016/j.renene.2011.07.034.

[13] B. Ni and C. Sourkounis, "Energy yield and power fluctuation of different control methods for wind energy converters," *IEEE Trans. Ind. Appl.*, vol. 47, no. 3, pp. 1480–1486, May/Jun. 2011. doi: 10.1109/TIA.2011.2126551.

[14] M. B. Smida and A. Sakly, "Smoothing wind power fluctuations by particle swarm optimization-based pitch angle controller," *Trans. Inst. Meas. Control*, vol. 41, no. 3, pp. 647–656, Feb. 2019. doi: 10.1177/0142331218764594.

[15] X. Lyu, J. Zhao, Y. Jia, Z, Xu, and K. P. Wong, "Coordinated control strategies of PMSG-based wind turbine for smoothing power fluctuations," *IEEE Trans. Power Syst.*, vol. 31, no. 1, pp. 391–401, Jan. 2019. doi: 10.1109/TPWRS.2018.2866629.

[16] G. Ren, J. Liu, J. Wan, Y. Guo, and D. Yu, "Overview of wind power intermittency: Impacts, measurements, and mitigation solutions," *Appl. Energy*, vol. 204, pp. 47–65, Oct. 2017. doi: 10.1016/j.apenergy.2017.06.098.

[17] Y. Uchida, G. Koshimizu, T. Nanahara, K. Yoshimoto, Y. Uchida, G. Koshimizu, T. Nanahara, K. Yoshimoto, "New control method for regulating state-of- charge of a battery in hybrid wind power/battery energy storage system," in *Proc. IEEE PES Power Syst. Conf. Expo.*, Atlanta, GA, USA, Oct./Nov. 2006, pp. 1244–1251.

[18] C. Kim, E. Muljadi, and C. Chung, "Coordinated control of wind turbine and energy storage system for reducing wind power fluctuation," *Energies*, vol. 11, no. 1, p. 52, Dec. 2017. doi: 10.3390/en11010052.

[19] D. Lamsal, T. Conradie, V. Sreeram, Y. Mishra, and D. Kumar, "Fuzzy-based smoothing of fluctuations in output power from wind and photovoltaics in a hybrid power system with batteries," *Int. Tran. Electr. Energy Syst.*, vol. 3, no. 3, p. e2757, Mar. 2019. doi: 10.1002/etep.2757.

[20] J. Li, R. Xiong, H. Mu, B. Cornélusse, P. Vanderbemden, D. Ernst, and W. Yuan, "Design and real-time test of a hybrid energy storage system in the microgrid with the benefit of improving the battery lifetime," *Appl. Energy*, vol. 218, pp. 470–478, May 2018. doi: 10.1016/j.apenergy.2018.01.096.

[21] Q. Jiang and H. Hong, "Wavelet-based capacity configuration and coordinated control of hybrid energy storage system for smoothing out wind power fluctuations," *IEEE Trans. Power Syst.*, vol. 28, no. 2, pp. 1363–1372, May 2013. doi: 10.1109/TPWRS.2012.2212252.

[22] X. Zhang, Y. Yuan, L. Hua, Y. Cao, and K. Qian, "On generation schedule tracking of wind farms with battery energy storage systems," *IEEE Trans. Sustain. Energy*, vol. 8, no. 1, pp. 335–341, Jan. 2017. doi: 10.1109/TSTE.2016.2598823.

[23] B. Kirby and E. Hirst, "Generator response to intrahour load fluctuations," *IEEE Trans. Power Syst.*, vol. 13, no. 4, pp. 1373–1378, Nov. 1998. doi: 10.1109/59.736279.

[24] W. Lin, J. Wen, X. Ai, S. Chen, and W. Li, "Probability density function of wind power variations," *Proc. CSEE*, vol. 32, no. 1, pp. 38–46, Jan. 2012.

[25] R. H. A. Zubo, G. Mokryani, and R. Abd-Alhameed, "Optimal operation of distribution networks with high penetration of wind and solar power within a joint active and reactive distribution market environment," *Appl. Energy*, vol. 220, pp. 713–722, Jun. 2018. doi: 10.1016/j.apenergy.2018.02.016.

[26] A. Carpinone, M. Giorgio, R. Langella, and A. Testa, "Markov chain modeling for very-short-term wind power forecasting," *Electr. Power Syst. Res.*, vol. 122, pp. 152–158, May 2015. doi: 10.1016/j.epsr.2014.12.025.

[27] F. Cadini, L. G. Agliardi, and E. Zio, "A modeling and simulation framework for the reliability/availability assessment of a power transmission grid subject to cascading failures under extreme weather conditions," *Appl. Energy*, vol. 140, pp. 267–279, Jan. 2017. doi: 10.1016/j.apenergy.2016.10.086.

XINSONG ZHANG received the B.E. degree in electrical engineering from the Xi'an University of Technology, Xi'an, China, in 2002, the M.Sc. degree in electrical engineering from Xi'an Jiaotong University, Xi'an, in 2005, and the Ph.D. degree from Hohai University, Nanjing, China, in 2013. He joined the Faculty of Nantong University, China, in 2006. From 2018 to 2019, he was an Academic Visitor with the Department of Electronic and Electrical Engineering, University of Bath, Bath, U.K. He is currently an Associate Professor with the School of Electrical Engineering, Nantong University. His research interests include power systems operation and planning, wind power integration, and energy storage systems.

JUPING GU received the Ph.D. degree in electrical engineering from Southeast University, Nanjing, China, in 2003. In 1995, she joined the Faculty of Nantong University, Nantong, China, where she is currently a Professor with the the School of Electrical Engineering. She is also the Vice President of Nantong University. Her research interests include power systems operation and planning, wind power integration, battery energy storage technologies, and control theory and its application.

LIANG HUA received the B.E. degree in electrical engineering from Nantong University, Nantong, China, in 2001, and the M.Sc. and Ph.D. degrees from the Zhejiang University of Technology in Control Engineering, Hangzhou, China, in 2008 and 2014, respectively. In 2001, he joined the Faculty of Nantong University, China, where he is currently a Professor and the Executive President of the School of Electrical Engineering. His research interests include power systems optimization, renewable power generation, and energy storage systems.

KANG MA received the B.Eng. degree from Tsinghua University, Beijing, China, in 2007, and the Ph.D. degree in electrical engineering from The University of Manchester, Manchester, U.K., in 2011. He was an Research and Development Engineer with the China Electric Power Research Institute, Beijing, from 2011 to 2014, during that time he developed the first version of the reliability assessment module for a distribution network planning platform. This platform has been widely applied to over 20 provincial grid companies in China. He is currently a Lecturer with the University of Bath, Bath, U.K. He has published six papers on phase imbalance in the IEEE TRANSACTIONS ON POWER SYSTEMS, covering the characteristics, consequences, and treatment of phase imbalance. His research interests include low-voltage (LV) distribution network operation and planning, and battery energy storage systems, especially phase imbalance in LV networks.